Eur. Phys. J. A **24**, 205–209 (2005)
DOI 10.1140/epja/i2004-10137-2

THE EUROPEAN PHYSICAL JOURNAL A

Lifetimes of proton unstable states in ^{113}I measured by the particle–X-ray coincidence technique

Z. Janas[1,a], L. Batist[2], R. Borcea[3], J. Döring[3], M. Gierlik[1], M. Karny[1], R. Kirchner[3], M. La Commara[4], S. Mandal[3], C. Mazzocchi[3,5], F. Moroz[2], S. Orlov[2], A. Płochocki[1], E. Roeckl[3], and J. Żylicz[1]

[1] Institute of Experimental Physics, Warsaw University, PL-00681 Warsaw, Poland
[2] St. Petersburg Nuclear Physics Institute, 188-350 Gatchina, Russia
[3] Gesellschaft für Schwerionenforschung, D-64291 Darmstadt, Germany
[4] Department of Physical Sciences, University "Federico II" and INFN, I-80126 Napoli, Italy
[5] Department of Physics, University of Tennessee, Knoxville, TN 37996, USA

Received: 30 November 2004 / Revised version: 2 February 2005 /
Published online: 8 March 2005 –
Communicated by D. Schwalm

Abstract. The β-delayed proton decay of ^{113}Xe was investigated by means of a total absorption γ-ray spectrometer and a telescope for particle detection. The energy window available for the β-delayed proton decay of ^{113}Xe and the relative branching ratios for proton transitions to the ^{112}Te states were remeasured. The lifetimes of proton unstable ^{113}I states populated in the electron capture decay of ^{113}Xe were determined by means of the particle–X-ray coincidence technique. The results of the lifetime measurements are compared with statistical-model calculations.

PACS. 23.40.-s β decay; double β decay; electron and muon capture

1 Introduction

It has been demonstrated that the particle–X-ray coincidence technique (PXCT) [1] can provide information on lifetimes of excited nuclear states in the time range of 10^{-15}–10^{-17} s, such data being difficult to access by other methods. The PXCT method uses an "atomic clock" (filling of the atomic shell vacancy) to measure the time scale of the nuclear de-excitation process. The technique can only be applied if a particle unstable nuclear state and an atomic shell vacancy are created simultaneously. The β-delayed proton (βp) emission following electron capture (EC) decay is ideally suited for this type of measurements. The principle of the method is illustrated in fig. 1: A nucleus (with atomic number Z) decaying, *e.g.*, by K-electron capture to the excited state in the daughter $(Z-1)$ produces simultaneously an atomic K-shell vacancy. If this level decays by proton emission, then, depending on whether the vacancy is filled before or after the proton emission, the X-rays related to the filling process are characteristic for $(Z-1)$ or $(Z-2)$ element, respectively.

For a single-proton transition, assuming that atomic and nuclear de-excitations are uncoupled and follow the exponential decay law, the relative intensity of the $(Z-2)$ and $(Z-1)$ KX-ray peaks ($I_{K\mathrm{X}}(Z-2)/I_{K\mathrm{X}}(Z-1)$) observed in coincidence with protons is related with the total widths of the nuclear level (Γ_{nucl}) and the K-shell vacancy state (Γ_K) via the formula $I_{K\mathrm{X}}(Z-2)/I_{K\mathrm{X}}(Z-1) = \Gamma_{\mathrm{nucl}}/\Gamma_K$ [2]. Since the total widths of the K-shell vacancy

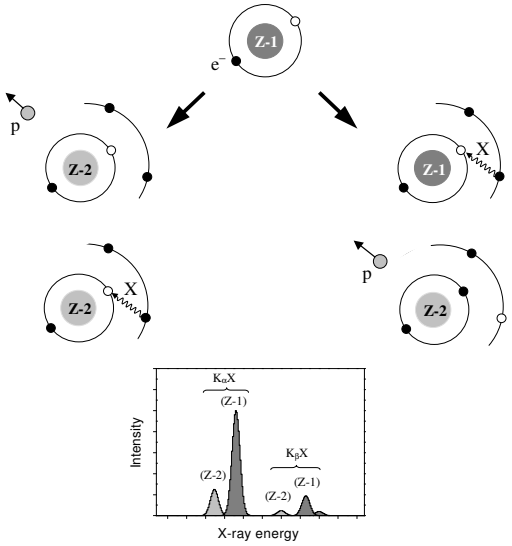

Fig. 1. Pictorial presentation of the PXCT method for lifetime measurements of proton-emitting states.

[a] e-mail: janas@mimuw.edu.pl

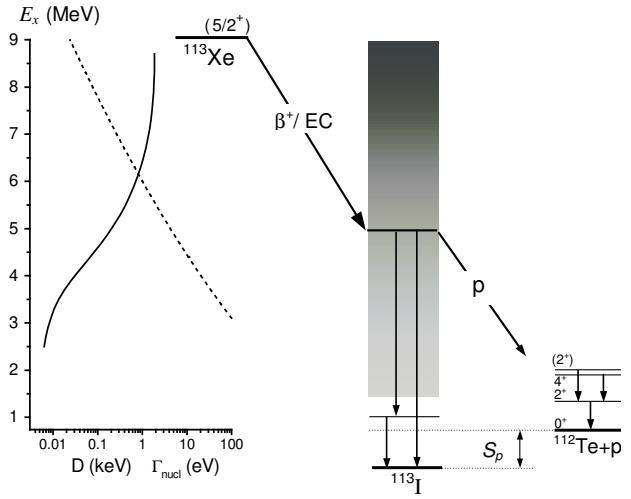

Fig. 2. Beta-delayed proton decay scheme of ^{113}Xe. On the left side of the figure the calculated average distance D (dashed line) and the total width $\Gamma_{\rm nucl}$ (solid line) of $I_i^\pi = 5/2^+$ states are shown as a function of ^{113}I excitation energy.

states are known [3,4], the $I_{KX}(Z-2)/I_{KX}(Z-1)$ ratio is a direct measure of the total decay width of the excited daughter state.

The same idea of particle–X-ray coincidence analysis is at the origin of the works of Chemin *et al.* [5] and Röhl *et al.* [6] reporting on the lifetime measurements of compound nuclear systems created in proton-induced reactions. This technique, although in principle more versatile being not dependent on the particular EC transition, is hampered by the uncertainties of theoretical and experimental estimates of the probability of simultaneous excitation of the atomic vacancy and nuclear resonance.

In this paper we report on a reinvestigation of the βp decay of ^{113}Xe by using the total absorption spectrometer (TAS) [7]. So far the decay of ^{113}Xe has been studied by Hagberg *et al.* [8] and Tidemand-Petersson *et al.* [9,10]. The ground-state α emission, the β-delayed proton and α-decay branches were investigated in these works. The half-life ($T_{1/2} = (2.74 \pm 0.08)$ s) and the spin and parity ($I^\pi = 5/2^+$) of ^{113}Xe were determined as well as the energy available for the proton emission ($Q_{\rm EC} - S_{\rm p} = (7920 \pm 150)$ keV) and the relative feeding of the ^{112}Te states populated by the βp transitions. Figure 2 shows the βp decay scheme of ^{113}Xe resulting from these works. Our study focused on the PXCT measurements which for the first time provided information on the lifetimes of the proton unstable states in ^{113}I, populated in the EC decay of ^{113}Xe. In addition, more reliable data on the $Q_{\rm EC} - S_{\rm p}$ value and on the relative βp feeding of the ^{112}Te states were obtained.

In the following, details of the present measurements of the ^{113}Xe βp decay will be outlined and the results obtained will be presented. The measured lifetimes of ^{113}I states will be compared with results of statistical-model calculations.

2 Experimental method

The ^{113}Xe nuclei were produced in the fusion-evaporation reactions of a 4.74 MeV/u ^{58}Ni beam impinging on a 3.7 mg/cm^2 thick ^{58}Ni target. Reaction products recoiling out of the target were stopped in a Nb/Ta catcher and ionized in the FEBIAD-B2-C [11] ion source of the GSI on-line mass separator. The ions extracted from the source were accelerated to 55 keV and mass-separated in a magnetic field. The $A = 113$ beam was implanted into a transport tape which periodically moved the collected activity into the center of the TAS [7]. The main part of the TAS is a large ($\varnothing$36 cm $\times$ 36 cm) NaI(Tl) crystal for γ-ray detection. A well along the crystal's symmetry axis accommodates an assembly of germanium X-ray detector, 600 μm thick silicon β-particle counter and telescope for β-delayed particle registration. The latter consisted of a 35 μm, 150 mm^2 ΔE silicon detector and a 550 μm, 450 mm^2 E silicon detector mounted 3 mm behind the ΔE counter. The radioactive sources were positioned in air between the β detector and the telescope placed at the distance of 1.5 mm from the tape. The βp energy spectra were obtained by summation of coincident ΔE and E signals, corrected for the average energy loss of protons in air [12]. The energy calibration of the TAS detectors was performed by using standard γ-ray sources (for the TAS crystal and X-ray detector), conversion electron lines (for the β and E detectors), ^{148}Gd α source (for the ΔE detector) as well as a precise pulse generator.

3 Results

3.1 Feeding of ^{112}Te states by proton emission

The TAS enables the identification of the final states populated in the βp decay by detecting γ-rays following proton transition. Moreover, the total absorption effect in the TAS allows one to discriminate between the EC and positron decay modes. These unique features of the TAS are illustrated in fig. 3 which shows the TAS spectrum measured in coincidence with protons emitted in the β-decay of ^{113}Xe. The four prominent peaks visible in the spectrum correspond to βp transitions to specific ^{112}Te levels: The 689 keV and 689 + 1022 keV peaks correspond to the βp decay to the first-excited state of ^{112}Te after EC (ECp) and positron (β^+p) decays, respectively. The 1022 keV energy shift between the ECp and β^+p peaks is due to the absorption of two 511 keV quanta from the annihilation of positrons emitted in the β^+p decay. The 1480 + 1022 keV line indicates the β^+p feeding of the 1476 keV and the 1484 keV ^{112}Te states which were reported in ref. [10] but could not be resolved in the TAS spectrum. The 1022 keV peak corresponds to proton transitions to the ^{112}Te ground state after positron decay of ^{113}Xe. In the case of the ECp decay to the ground state of the final nucleus, no signal from the TAS crystal is detected.

The βp-gated TAS spectrum was decomposed into contributions from the β^+p and ECp transitions to individual final states [10] by fitting the simulated TAS response

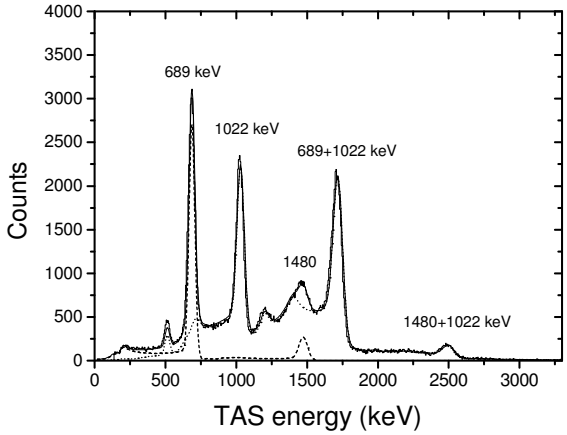

Fig. 3. TAS γ-ray spectrum gated by βp from ^{113}Xe decay. Experimental data (histogram) are compared with the results of simulations. The dotted and dashed lines indicate components corresponding to β^+p and ECp transitions, respectively.

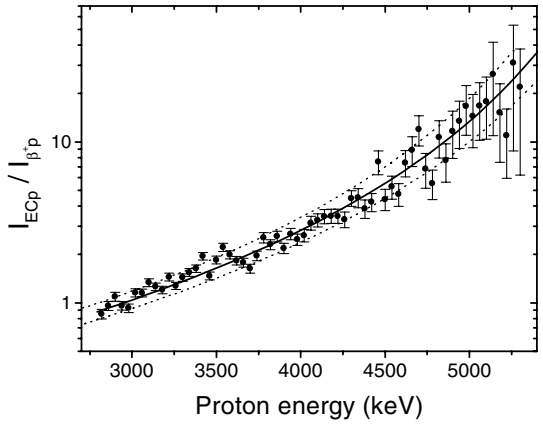

Fig. 4. The $I_{\mathrm{ECp}}/I_{\beta^+\mathrm{p}}$ ratio as a function of proton energy in the ^{113}Xe βp decay to the first-excited 2^+ state in ^{112}Te. The solid line represents the best fit of the theoretical $I_{\mathrm{ECp}}/I_{\beta^+\mathrm{p}}$ ratio to the data points, yielding a $Q_{\mathrm{EC}}-S_{\mathrm{p}}$ value of 8300 keV. The dotted lines indicate the $I_{\mathrm{ECp}}/I_{\beta^+p}$ ratio calculated for the $Q_{\mathrm{EC}}-S_{\mathrm{p}}$ changed by the standard deviation of $\pm$150 keV.

Table 1. Experimentally determined relative branching ratios for the βp decay of the ^{113}Xe to ^{112}Te states.

^{112}Te levels		βp branching ratio (%)	
E_f (keV)	I^π	This work	ref. [10]
0	0^+	32 ± 2	47 ± 5
689	2^+	60 ± 3	46 ± 5
1476	4^+	8 ± 1	3.8 ± 0.7
1484	(2^+)		3.3 ± 0.6

functions [13]. As illustrated in fig. 3, a very good description of the βp-gated TAS spectrum was achieved. Table 1 shows the relative branching ratios for (β^+p + ECp) transitions to the ^{112}Te states, as obtained by the fitting procedure. We note that the feeding of the ^{112}Te ground state is almost two times lower than the feeding of the first-excited 2^+ state. This result disagrees with the βp decay scheme of ^{113}Xe proposed in ref. [10], where equal intensities of proton transitions to the ground state and 689 keV level are indicated. The reason for this discrepancy is difficult to identify. However, we point out that in view of the perfect description of the measured βp-gated TAS spectrum (see fig. 3), the systematic uncertainties of the branching ratios determined in this work are apparently negligible.

3.2 Determination of the $Q_{EC} - S_p$ value

For the selected final state, the intensity ratio of the ECp and β^+p spectra ($I_{\mathrm{ECp}}/I_{\beta^+\mathrm{p}}$) plotted as a function of the energy of emitted particles depends only on the energy window open for the βp decay and can thus be used to determine the $Q_{\mathrm{EC}}-S_{\mathrm{p}}$ energy difference. Figure 4 shows the $I_{\mathrm{ECp}}/I_{\beta^+\mathrm{p}}$ ratio as a function of proton energy in the decay of ^{113}Xe to the first-excited 2^+ state in ^{112}Te. The respective proton spectra were obtained by setting the gate condition on the 689 and the 689 + 1022 keV lines in the TAS spectrum (see fig. 3). To avoid summation of the proton and positron signals, the β^+p spectrum was additionally gated by the β-particles registered in the silicon detector opposite to the ΔE-E telescope. The measured spectra were corrected for the gate efficiencies. The latter quantities were extracted from the simulated TAS response functions for the ECp and the β^+p decay to the 689 keV ^{112}Te state. The experimental data points were fitted by the theoretical ratio of the statistical rate function for β^+ emission and EC decay [14]. The $Q_{\mathrm{EC}}-S_{\mathrm{p}}$ energy difference was the only free parameter in the χ^2 minimization procedure which yielded the $Q_{\mathrm{EC}}-S_{\mathrm{p}}$ value of (8300$\pm$150) keV. This value is 380 keV higher than the $Q_{\mathrm{EC}}-S_{\mathrm{p}}$ energy difference reported by Tidemand-Petersson *et al.* [10].

Although in both measurements the $Q_{\mathrm{EC}}-S_{\mathrm{p}}$ value was determined with the same accuracy, we consider our result as more reliable. The method applied in ref. [10] relied, to some extent, on statistical-model calculations, implying assumptions to be made, *e.g.*, on the shape of the β-strength function. The latter was adjusted to reproduce the measured βp branching ratios which are questioned by our results (see sect. 3.1). In our measurement the proton spectra corresponding to the transitions to the specific ^{112}Te state were selected and the $I_{\mathrm{ECp}}/I_{\beta^+\mathrm{p}}$ ratio was calculated in a model-independent way.

The $Q_{\mathrm{EC}}-S_{\mathrm{p}}$ value determined in this work, together with the known ^{113}Xe Q_{EC} value of (9040 $\pm$ 100) keV [15] yields (740$\pm$180) keV for the proton separation energy of ^{113}I.

3.3 Proton–X-ray coincidence measurement

The PXCT measurement for the ^{113}Xe decay was performed by selecting ECp transitions to the ^{112}Te 2^+ state. This final state was specified by setting the energy gate on the 689 keV line visible in the proton-gated TAS spectrum (see fig. 3). The inset in fig. 5 shows the X-ray spectrum

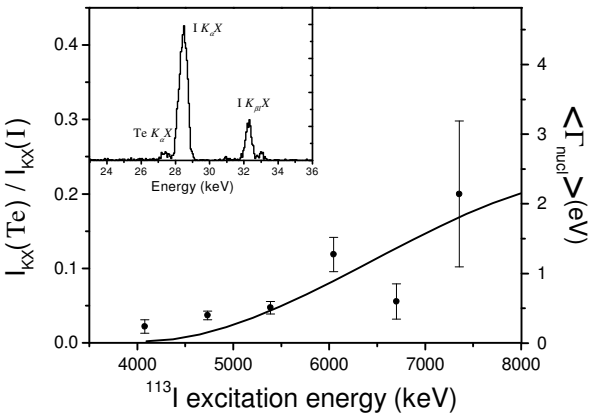

Fig. 5. The $I_{KX}(\mathrm{Te})/I_{KX}(\mathrm{I})$ ratio for proton transitions to the ^{112}Te 2^+ state plotted in 650 keV intervals as a function of ^{113}I excitation energy. The solid line shows the result of the statistical-model calculations (see sect. 4 for details). The inset shows the X-ray spectrum gated by protons and the 689 keV γ transition registered in the TAS.

Table 2. The $I_{KX}(\mathrm{Te})/I_{KX}(\mathrm{I})$ ratio for proton transitions to the ^{112}Te 2^+ state measured in selected ^{113}I excitation energy intervals. In the last column the corresponding average total widths $\langle\Gamma_{\mathrm{nucl}}\rangle$ of ^{113}I states are given.

E_x (MeV)	$I_{KX}(\mathrm{Te})/I_{KX}(\mathrm{I})$	$\langle\Gamma_{\mathrm{nucl}}\rangle$ (eV)
3.75–4.40	0.022 ± 0.009	0.23 ± 0.10
4.40–5.05	0.037 ± 0.006	0.40 ± 0.06
5.05–5.70	0.047 ± 0.008	0.5 ± 0.1
5.70–6.35	0.12 ± 0.02	1.3 ± 0.3
6.35–7.00	0.06 ± 0.02	0.6 ± 0.2
7.00–7.65	0.20 ± 0.10	2.1 ± 1.1

registered in coincidence with protons (unrestricted in energy) and the 689 keV line recorded in the TAS. The tellurium and iodine KX-ray peaks are clearly visible, their intensity ratio ($I_{KX}(\mathrm{Te})/I_{KX}(\mathrm{I})$) being (5.2±0.5)%. We note that this value is 3–5 times lower than the typical PXCT ratio measured for isotopes in the $A = 65$–80 region [1,16,17].

Table 2 and fig. 5 show the measured $I_{KX}(\mathrm{Te})/I_{KX}(\mathrm{I})$ ratio as a function of ^{113}I excitation energy. The latter was calculated as $E_x = A/(A-1)E_\mathrm{p} + S_\mathrm{p} + E_f$, where A is the precursor mass number, E_p is the kinetic energy of protons emitted to the ^{112}Te state with excitation energy E_f and S_p is the proton separation energy in ^{113}I, respectively. Knowing that the total width of the K-shell vacancy state in the iodine atom is 10.7 eV [3,4] one can calculate the corresponding average total widths of the ^{113}I states. As shown on the scale on the right side of fig. 5, in the excitation energy range of 3.8–7.7 MeV the total widths of ^{113}I states populated in the ECp decay of the ^{113}Xe $5/2^+$ state increase from $\sim$ 0.2 to $\sim$ 2 eV. The corresponding lifetimes range from $3.3 \cdot 10^{-15}$ to $3.3 \cdot 10^{-16}$ s. We note that the indicated widths (lifetimes) are averaged over 650 keV ^{113}I excitation energy intervals and must be regarded as averages over states with spins that are allowed to be populated in the decay of ^{113}Xe (see sect. 4).

4 Statistical-model calculations

The investigations of βp emitters in the *trans*-tin region [10] indicated that the statistical model [18,19] can be successfully used to explain properties of measured β-delayed particle spectra. This conclusion is, however, biased by the assumptions which in most cases had to be made regarding the shape of the β-strength function governing the β-decay process. In fact the β-strength distributions were adjusted to reproduce the measured energy spectra and branching ratios as, *e.g.*, was done in the case of studies of the ^{113}Xe [10].

Our PXCT measurements provide information on the average lifetime of ^{113}I excited states, which allowed us to test the ability of the statistical model to describe the evolution of the total decay width with the excitation energy without making any assumptions on the shape of the β-strength distribution.

In the statistical model the βp decay is treated as a two-step process. In the first step the βp precursor with spin and parity $I_0^{\pi_0}$ decays via allowed, in the case of ^{113}Xe decay, β^+/EC transitions and populates states with spins and parities $I_i^{\pi_i} = I_0^{\pi_0}, I_0^{\pi_0} \pm 1$ in the intermediate nucleus. It is assumed that the intermediate states are populated with a probability proportional to $(2I_i + 1)$, which is the number of spin I_i projections.

The second step is the de-excitation process of the states populated in β-decay. It may proceed via γ-ray or particle (protons, α-particles) emission. The radiation widths of the levels are calculated by using the statistical model of nuclear electromagnetic de-excitation [20]. The $E1$-, $M1$- and $E2$-type transitions were considered in our calculations and the respective decay widths were obtained by using the γ-strength function models proposed by Kopecky *et al.* [21]. The proton widths for intermediate states decaying to the ground state and excited levels of the final nucleus were calculated according to the prescription given in ref. [18]. We used the barrier transmission coefficients for protons calculated with the set of optical-model potential parameters proposed by Johnson *et al.* [22].

The plot on the left side of fig. 2 shows the total widths (Γ_{nucl}) of $I_i^\pi = 5/2^+$ states calculated as a function of ^{113}I excitation energy. The same plot shows the average distance of $5/2^+$ states in ^{113}I obtained with the back-shifted Fermi-gas model level density formula [23] which was consistently applied in the calculations of the radiative and proton decay widths. The level density parameter $a = 14.9$ MeV^{-1} was adopted following the systematic trends in the $A = 110$–130 mass region [23]. Another parameter, the fictive ground-state position Δ, was adjusted to reproduce the energy dependence of the total level width resulting from the PXCT measurement. In the calculations the modification of the exponential decay law due to the Porter-Thomas fluctuation of the partial proton decay widths was taken into account [2]. The solid line

in fig. 5 shows the $I_{KX}(\mathrm{Te})/I_{KX}(\mathrm{I})$ ratio calculated as a function of ^{113}I excitation energy for $\Delta = 1.1$ MeV for which reasonable agreement between the measured and calculated PXCT ratios was obtained.

5 Summary

In summary, the βp decay of ^{113}Xe was studied at the GSI on-line mass separator by using the TAS spectrometer equipped with the X-ray detector and the telescope for βp registration. The very high efficiency of the TAS enabled the selection of the βp decay branches to specific final states without substantial losses in the counting statistics. This possibility considerably facilitated the analysis and interpretation of the data. Measurements of the γ-p coincidences provided reliable information on the feeding of the ^{112}Te excited states in the βp decay of ^{113}Xe. The energy window open for the βp decay of ^{113}Xe to the first-excited ^{112}Te 2^+ state was measured and used to determine the $Q_{\mathrm{EC}} - S_{\mathrm{p}}$ energy difference without making assumptions on the shape of the β-strength distribution. The PXCT measurements for ^{113}Xe were performed and, for the first time, information on the average total width of ^{113}I excited states was obtained. The measured excitation energy dependence of the average level lifetimes was reasonably well reproduced by statistical-model calculations with adjusted level density parameters.

The authors are thankful to K. Burkard and W. Hüller for their assistance in the operation of the GSI on-line mass separator.

References

1. J.C. Hardy *et al.*, Phys. Rev. Lett. **37**, 133 (1976).
2. P. Asboe-Hansen *et al.*, Nucl. Phys. A **361**, 23 (1981).
3. J.H. Scofield, *Atomic Inner-Shell Processes*, edited by B. Crasemann (Academic Press, New York, 1975) p. 265.
4. W. Bambynek *et al.* Rev. Mod. Phys. **44**, 716 (1972).
5. J.F. Chemin *et al.*, Nucl. Phys. A **331**, 407 (1979).
6. S. Röhl, S. Hoppenau, M. Dost, Phys. Rev. Lett. **43**, 1300 (1979).
7. M. Karny *et al.*, Nucl. Instrum. Methods B **126**, 411 (1997).
8. E. Hagberg *et al.*, Nucl. Phys. A **208**, 309 (1973).
9. P. Tidemand-Petersson, A. Płochocki, Phys. Lett. B **118**, 278 (1982).
10. P. Tidemand-Petersson *et al.*, Nucl. Phys. A **437**, 342 (1985).
11. R. Kirchner *et al.*, Nucl. Instrum. Methods **234**, 224 (1985).
12. J.P. Biersack, J.F. Ziegler, SRIM 2000, `http://www.SRIM.org`.
13. GEANT: Detector description and simulation tool, CERN, Program Library W5013, Geneva, 1994.
14. N.B. Gove, M.J. Martin, Nucl. Data Tables A **10**, 205 (1971).
15. G. Audi, A.H. Wapstra, C. Thibault, Nucl. Phys. A **729**, 337 (2003).
16. P. Asboe-Hansen *et al.*, Phys. Lett. B **77**, 363 (1978).
17. J. Giovinazzo *et al.*, Nucl. Phys. A **674**, 394 (2000).
18. P. Hornshøj *et al.*, Nucl. Phys. A **187**, 609 (1972).
19. B. Jonson *et al.*, in *Proceedings of the Third International Conference on Nuclei Far from Stability, Cargèse, 1976*, CERN 76-13 (CERN, Geneva, 1976) p. 277.
20. G.A. Bartholomew *et al.*, Adv. Nucl. Phys. **7**, 229 (1973).
21. J. Kopecky, M. Uhl, Phys. Rev. C **41**, 1941 (1990).
22. C.H. Johnson *et al.*, Phys. Rev. C **20**, 2052 (1979).
23. W. Dilg, W. Schantl, H. Vonach, M. Uhl, Nucl. Phys. A **217**, 269 (1973).